

How Does a Deep Learning Model Architecture Impact Its Privacy? A Comprehensive Study of Privacy Attacks on CNNs and Transformers

Guangsheng Zhang¹ Bo Liu¹ Huan Tian¹ Tianqing Zhu¹
Ming Ding² Wanlei Zhou³

¹University of Technology Sydney ²Data 61, CSIRO, Australia ³City University of Macau

Abstract

As a booming research area in the past decade, deep learning technologies have been driven by big data collected and processed on an unprecedented scale. However, privacy concerns arise due to the potential leakage of sensitive information from the training data. Recent research has revealed that deep learning models are vulnerable to various privacy attacks, including membership inference attacks, attribute inference attacks, and gradient inversion attacks. Notably, the efficacy of these attacks varies from model to model. In this paper, we answer a fundamental question: *Does model architecture affect model privacy?* By investigating representative model architectures from CNNs to Transformers, we demonstrate that Transformers generally exhibit higher vulnerability to privacy attacks compared to CNNs. Additionally, We identify the micro design of activation layers, stem layers, and LN layers, as major factors contributing to the resilience of CNNs against privacy attacks, while the presence of attention modules is another main factor that exacerbates the privacy vulnerability of Transformers. Our discovery reveals valuable insights for deep learning models to defend against privacy attacks and inspires the research community to develop privacy-friendly model architectures.

1 Introduction

Deep learning has been gaining massive attention over the past several years. Training deep learning models requires the collection and processing of user data, which raises significant privacy concerns. The data gathered during the training phase often contains sensitive information that can potentially be accessed or retrieved by malicious parties. Various privacy attacks targeting deep learning models have demonstrated this vulnerability extensively. One prominent type of attack is membership inference, which focuses on determining whether a specific data sample belongs to the training data [46, 48]. Another attack is attribute inference, which aims to uncover implicit attributes learned by the model beyond the intended

target attribute [40, 51]. Additionally, gradient inversion attacks pose a significant threat by attempting to reconstruct the information of the training data from the gradients of the model [12, 13]. These attacks enable adversaries to exploit deep learning models to extract sensitive data.

Prior research has established that overfitting is one of the primary causes of privacy leakage in deep learning models [6, 17, 31, 48]. In general, overfitting occurs when models excessively learn specific details from the training data, which can lead to inadvertent privacy breaches. Surprisingly, even when models exhibit comparable levels of overfitting, the effectiveness of attacks varies across different models. This observation raises intriguing questions as to why certain deep learning models are more susceptible to privacy attacks compared to others, a puzzle that researchers have not fully comprehended. Consequently, we conjecture that other factors beyond overfitting might also contribute to the increased vulnerability of some deep learning models to privacy attacks. Thus, this paper aims to answer the following question: *How does a model's architecture affect its privacy preservation capability?*

In this paper, we answer this question by conducting a comprehensive analysis of different deep learning models under a variety of state-of-the-art privacy attacks. Our investigation focuses on two widely adopted deep learning model architectures: convolutional neural networks (CNNs) and Transformers. CNN-based models have been dominant in computer vision, thanks to its sliding-window strategy to extract local information from images effectively. Transformers, initially introduced in natural language processing (NLP), have gained popularity in computer vision by capturing large receptive fields through attention mechanisms, resulting in comparable accuracy performance against CNNs. The tremendous achievements and wide usage of these two architectures provide us with a good opportunity to make a comparative analysis regarding model privacy risks. Through our investigation, we make an intriguing discovery: *Transformers, in general, exhibit higher vulnerability to mainstream privacy attacks compared to CNNs.*

While Transformers and CNNs have different designs from many perspectives, we further investigate whether there are some key designs in the model that have a major impact on privacy risks. To this end, we investigate which module leads to more privacy leakage in a Transformer architecture. We evaluate the privacy leakage of several major modules by sending only selected gradients to the gradient inversion attacks and discover that attention modules cause significant privacy leakage. Moreover, we start with a popular CNN-based model, ResNet-50 [16], and gradually morph the model to incorporate the key designs of Transformers. This leads us to the structure of ConvNeXt [34]. We evaluate the privacy leakage through this process and identify several key components that have a significant impact on privacy risks: (1) the design of the activation layers; (2) the design of stem layers; (3) the design of LN layers. We further conduct ablation studies to verify our discoveries and propose solutions to exploit the discoveries.

In summary, our contributions in this paper are summarized as follows:

- For the first time, we investigate the impact of model architectures and micro designs on privacy risks.
- We evaluate the privacy vulnerabilities of two widely-adopted model architectures, i.e., CNNs and Transformers, using three prominent privacy attack methods: (1) membership inference attacks, (2) attribute inference attacks, and (3) gradient inversion attacks. Our analysis reveals that Transformers exhibit higher vulnerabilities to these privacy attacks compared to CNNs.
- We identify three key factors: (1) the design of activation layers, (2) the design of stem layers, and (3) the design of LN layers, contribute to the enhanced resilience of CNNs in comparison to Transformers. We also discover that the presence of attention modules in Transformers could make them vulnerable to privacy attacks.
- We propose solutions to mitigate the vulnerabilities of model architectures: modifying model components and adding perturbations as defense mechanisms.

2 Related Work

2.1 Convolutional Neural Networks (CNNs)

Convolutional Neural Networks (CNNs) are a type of neural network that employs convolutional layers to extract features from input data. In contrast to fully connected networks, CNNs use convolutional kernels to connect small samples to neurons for feature extraction, reducing the number of model parameters and enabling the recognition of local features. Various techniques are employed to construct a CNN model, including padding, pooling, dilated convolution, group convolution, and more.

The idea of convolutional neural networks (CNNs) dates back to the 1980s [28]. However, the invention of AlexNet [27] makes CNNs the most prominent networks in computer vision. Subsequent research improved the accuracy and efficiency of models [49, 54]. ResNet [16] addressed the challenge of training deep networks using skip connections. Other notable networks consist of Inception [55], MobileNet [20], ResNeXt [62], RegNet [43], ConvNeXt [34].

2.2 Vision Transformers

Originating from natural language processing, Vision Transformers divide the input image into multiple patches, forming a one-dimensional sequence of token embeddings. Their exceptional performance can be attributed to the multi-head self-attention modules [59]. The attention mechanism has significantly contributed to the advancement of natural language processing [3, 9, 63], subsequently leading to the introduction of Transformers in the field of computer vision as Vision Transformers (ViT) [10]. Research by [10, 53] has shown that ViTs can surpass CNNs in various downstream tasks. Later research has focused on numerous improvements of ViTs, including tokenization [66], and position encoding [33]. Other advancements consist of lightweight Transformers in DeiT [56] and the "sliding windows" strategy in Swin Transformers [33].

Numerous studies have compared CNNs and Transformers from the perspectives of robustness [2, 42] and explainability [44]. However, our research diverges from previous works by concentrating on the privacy leakage inherent in both CNNs and Transformers.

2.3 Privacy Attacks on Deep Learning Models

A primary concern in deep learning privacy is that the model may reveal sensitive information from the training dataset. An adversary can predict whether a particular sample is in the model's training dataset via membership inference attacks, or disclose the implicit attributes of data samples via attribute inference attacks, or even recover private data samples utilized in training a neural network through gradient inversion attacks.

Membership inference attacks were initially introduced in [48], where an attack model was employed to distinguish member samples from non-member samples in the training data. To execute these attacks, shadow models mimic the behavior of victim models [46, 48]. Prediction results from victim models are gathered for attack model training. Usually, the confidence scores or losses were utilized [48], but more recent work (label-only attacks) applied prediction labels to launch attacks successfully [7, 29]. The attacks can also be executed by designing a metric with a threshold by querying the shadow model [52]. Some researchers expanded the attacks into new domains, including generative models [5, 15], se-

mantic segmentation [18, 67], federated learning [41, 58], and transfer learning [50, 74]. Other researchers relaxed the attack assumptions and improve the attacks. A black-box access is enough for membership inference [45]. A balanced accuracy is not an optimal metric for the attacks. Providing an ROC curve and the true positive rate at a low false positive rate can better measure the attack performance [4, 24, 36, 61, 64]. We select [4, 46, 48] as our baseline methods.

Attribute inference attacks, another significant category of privacy attack methods, attempt to reveal a specific sensitive attribute of a data sample by analyzing the representation of the victim model trained by the victim dataset. Melis et al. [40] presented the first attribute inference attack against deep learning models, which can be adopted in federated learning settings. Song and Shmatikov [51] later claimed that the overlearning feature of deep learning models caused the execution of the attacks. Attributes could also be inferred through a relaxed notion [71], model explanations [11], label-only settings [39], or imputation analysis [23]. As we aim to infer attributes from visual data, we select [40, 51] as baseline methods.

Gradient inversion attacks primarily aim to reconstruct training samples at the local clients in federated learning. Using the publicly shared gradients in the server, adversaries can execute the attacks by reconstructing the training samples using gradient matching. DLG [73] and its variant, iDLG [72], were the early attacks to employ an optimization-based technique to reconstruct the training samples. Later research like Inverting Gradients [13] and GradInversion [65] improved the attack performance by incorporating regularizations into the optimization process. APRIL [37] and GradViT [14] further developed the attack methods to extract sensitive information from Transformers. The use of Generative Adversarial Networks (GANs) in some gradient inversion attack methods [30] can have a significant impact on reconstructed results, making it difficult to isolate the influence of other factors on privacy leakage. Therefore, we use conventional gradient inversion attack methods [13] that do not involve the use of GANs.

There have been several evaluations and reviews of these privacy attacks against deep learning models [17, 21, 31, 32, 52, 68, 70]. However, we aim to evaluate the model architectures leveraging these privacy attacks. To sum up, we utilize conventional privacy attacks [4, 13, 40, 46, 48, 51] as the baseline attacks in our analysis, for these attack methods have inspired many follow-up research works, and they are suitable for evaluation on various models and datasets.

3 Methodology of Evaluating the Impact of the Model Architecture on Privacy

In this section, we present our approach to assessing the impact of model architectures on privacy leakage. In order to organize our study in a thorough and logical manner, We aim

to answer the following questions sequentially:

- RQ1: How to analyze the privacy leakage in model architectures?
- RQ2: What model architectures should we choose for the evaluation of these attacks?
- RQ3: What aspects should we focus on when evaluating the privacy attacks on model architectures?
- RQ4: How should we investigate what designs in model architectures contribute to privacy leakage?

In this work, we focus on classifier or feature representation models such as CNNs and Transformers, which are subject to the investigated privacy attacks. A new line of generative AI models, such as generative adversarial networks (GANs) and diffusion models, are vulnerable to different privacy attacks, and thus out of the scope of this paper. We believe the methodology of our evaluation could shed light on the effect of model privacy from the perspective of model architectures.

3.1 Privacy Threat Models

To answer the first research question, we choose three prominent privacy attack methods: membership inference attacks, attribute inference attacks, and gradient inversion attacks.

3.1.1 Membership Inference Attacks

Network-Based Attacks. Initiating a network-based membership inference attack [46, 48] requires three models: the victim model \mathcal{V} (the target of the attack), the shadow model \mathcal{S} (the model to mimic the behavior of the victim model), and the attack model \mathcal{A} (the classifier to give results whether the sample belongs to the member or non-member data). The following paragraphs provide explanations of how the attacks work.

The first step is the attack preparation. Since the adversary has only black-box access to the victim model \mathcal{V} , they can only query the model and record prediction results. To launch a membership inference attack, the adversary needs to create a shadow model \mathcal{S} , which behaves similarly to the victim model \mathcal{V} . This involves collecting a shadow dataset \mathcal{D}_S , which is usually a dataset from the same data distribution as the victim dataset \mathcal{D}_V . The shadow dataset \mathcal{D}_S is then divided into two subsets: \mathcal{D}_S^{train} for training and \mathcal{D}_S^{test} for testing.

Once the preparation is complete, the adversary trains attack model. The shadow model \mathcal{S} and shadow dataset \mathcal{D}_S are used to train the attack model \mathcal{A} . Each prediction result of a data sample from the shadow dataset \mathcal{D}_S is a vector of confidence scores for each class, which is concatenated with a binary label indicating whether the prediction is correct or not. The resulting vector, denoted as \mathcal{P}_S^i , is collected for all n samples, forming the input set $\mathcal{P}_S = \{\mathcal{P}_S^i, i = 1, \dots, n\}$ for the attack model \mathcal{A} . Since \mathcal{A} is a binary classifier, a three-layer MLP (multi-layer perceptron) model is employed to train it.

At last, the adversary launches the attack model inference. The adversary queries the victim model \mathcal{V} with the victim dataset \mathcal{D}_V and records the prediction results, which are used as the input for the attack model \mathcal{A} . The attack model then predicts whether a data sample is a member or non-member data sample.

Likelihood-Based Attacks. The Likelihood Ratio Attack (LiRA) [4] is a state-of-the-art attack method that employs both model posteriors and their likelihoods based on shadow models. In contrast to other attacks that rely on a single shadow model, LiRA requires the adversary to train multiple shadow models $\mathcal{S} = \{S_1, \dots, S_n\}$. This ensures that a target sample (from the victim dataset \mathcal{D}_V) is included in half of the models \mathcal{S} and excluded from the other half. The adversary then queries the shadow models with the target sample and calculates the logits for each model. Using these logits, the adversary calculates the probability density function to determine the likelihood ratio of the target sample, which corresponds to its membership status.

There are other kinds of membership inference attacks, including metric-based attacks and label-only attacks. Instead of using a neural network to be the attack model, metric-based attacks [52] launch the attacks using a certain metric and threshold to separate member data from non-member data. Label-only attacks [7, 29] relax the assumptions of the threat model leveraging only prediction labels as the input of the attack model. Our study focuses on two types of membership inference attacks: network-based and likelihood-based attacks. The reason we chose these two types of attacks is that the network-based attack is commonly used as a baseline in many research papers, making it a conventional attack to consider. Additionally, the likelihood-based attack is a more recent state-of-the-art attack that has demonstrated high effectiveness, making it an important attack to evaluate as well. By considering these two types of attacks, we can effectively represent the performance of membership inference attacks against various victim models and gain insights into potential privacy risks associated with different machine learning models.

3.1.2 Attribute Inference Attacks

The goal of attribute inference attacks [40, 51] is to extract sensitive attributes from a victim model, which may inadvertently reveal information about the training data. For instance, suppose the victim model is trained to classify whether a person has a beard or not. In that case, an adversary may infer the person’s race based on the model’s learned representation.

At the attack preparation stage, the victim model \mathcal{V} is trained by the victim dataset \mathcal{D}_V with two subsets \mathcal{D}_V^{rain} and \mathcal{D}_V^{test} for the training and testing.

The second step is also the attack model training. To train the attack model \mathcal{A} , the adversary uses an auxiliary dataset \mathcal{D}_A^{rain} , which includes pairs of the representation h and the

attribute a , i.e., $(h, a) \in \mathcal{D}_A$.

At last, the adversary launches the attack. The adversary takes a data sample’s representation h as the input and uses the attack model \mathcal{A} to infer the attribute result.

3.1.3 Gradient Inversion Attacks

Launching the gradient inversion attack [13, 72, 73] involves solving an optimization problem, which aims to minimize the difference between the calculated model gradients and the original model gradients. The optimization process continues for a certain number of iterations, after which the input data sample can be reconstructed.

The adversary operates within a federated learning scenario. In the attack preparation stage, the adversary operates from the central server, where model gradients are aggregated to create a centralized model. Since the adversary has access to the communication channels used during the federated learning process, they can retrieve the model gradients and prepare to extract sensitive information from the training samples. This allows the adversary to launch attacks against the federated learning system.

In the step of gradient reconstruction, the aggregated model gradients are denoted as $\nabla_{\theta} \mathcal{L}_{\theta}(x, y)$, where θ is the model parameters, x and y are the original input image and its ground truth in a local client, and \mathcal{L} represents the cost function for the model. To initiate the reconstruction process, the adversary generates a dummy image x^* . The adversary tries to minimize this cost function: $\arg \min_x \|\nabla_{\theta} \mathcal{L}_{\theta}(x, y) - \nabla_{\theta} \mathcal{L}_{\theta}(x^*, y)\|^2$. The dummy image x^* is reconstructed to resemble x closely.

3.2 CNNs vs Transformers

To answer the second research question, we investigate the privacy of two mainstream architectures: CNNs and Transformers. We carefully select several popular CNNs and Transformers for the attacks to analyze the privacy leakage.

For CNNs, we choose ResNets [16] as baseline models, which are known for their incorporation of residual blocks and have become widely used in various computer vision tasks. We specifically select ResNet-50 (23.52 million parameters) and ResNet-101 (42.51 million parameters) to represent CNN architectures in our analysis. Regarding Transformers, we focus on Swin Transformers [33], which have gained attention for their innovative design incorporating attention modules and shifted window mechanisms. We analyze Swin-T (27.51 million parameters) and Swin-S (48.80 million parameters) as representatives of Transformer architectures.

To ensure a fair comparison, we organize the evaluation of the four models based on their parameter sizes, grouping models with similar parameter sizes together. This approach allows us to compare models that exhibit comparable task performances while considering their architectural differences. Specifically, we compare ResNet-50 with Swin-T, as they

Table 1: Training recipes for privacy attacks.

Config	Hyperparameter
for all models of membership inference	
optimizer	AdamW
learning rate	0.001
weight decay	0.05
optimizer momentum	$\beta_1, \beta_2 = 0.9, 0.999$
batch size	256
training epochs	300
learning rate schedule	cosine annealing
mixup	0.8
cutmix	1.0
label smoothing	None
for all models of attribute inference	
optimizer	SGD
learning rate	0.01
weight decay	0.0005
optimizer momentum	0.9
batch size	256
training epochs	100
random augmentation	None
for gradient inversion	
cost function	similarity
optimizer	Adam
learning rate	0.1
total iteration	3000
total variance	0.0001

have similar parameter sizes, and we compare ResNet-101 with Swin-S for the same reason.

Apart from model architectures, training Transformers requires a modernized training procedure compared to training traditional CNNs. In order to make fair comparisons, we apply the same training recipe for CNNs and Transformers in each comparison.

4 Evaluation on Privacy Attacks with CNNs and Transformers

In this section, we address the third research question and provide a comprehensive analysis of the experimental settings and results. We aim to compare the attack performance under various metrics to gain a deeper understanding of the findings.

4.1 Settings

Datasets. Our experiments evaluate the privacy leakage under these five datasets.

- **CIFAR10 [26]** consists of 60,000 color images with dimensions of 32×32 pixels. It is organized into ten classes, with each class containing 6,000 images. The dataset covers a wide range of general object categories.
- **CIFAR100 [26]** is similar to CIFAR10 but with 100 classes. Each class has 600 images and represents a specific general object category.

- **ImageNet1K [8]** is a widely used dataset in computer vision containing over 1 million labeled images, covering 1,000 different classes. The dataset encompasses a diverse range of objects and scenes.
- **CelebA [35]** contains over 200,000 face images, each with 40 binary attributes.

In membership inference attacks, we use two datasets: CIFAR10, and CIFAR100. For network-based attacks, each dataset is evenly split into four subsets for training and testing both the victim and shadow models to ensure a fair evaluation. For likelihood-based attacks, we follow the training settings in [4].

For attribute inference attacks, we utilize the CelebA dataset, which provides rich attribute labeling. This allows us to accurately identify hidden attributes. In our experiments, we focus on inferring the race attribute while using the gender attribute as the classification goal for the victim model. We randomly select 20,000 images from CelebA and evenly split them into four subsets for training and testing both the victim model and the attribute inference attack model.

In gradient inversion attacks, we employ the CIFAR10 and ImageNet1K datasets. These attacks are conducted in a federated learning scenario, aiming to reconstruct the training batch. To evaluate the attacks, we randomly select a subset of images from these datasets, ensuring a representative assessment of the attack performance.

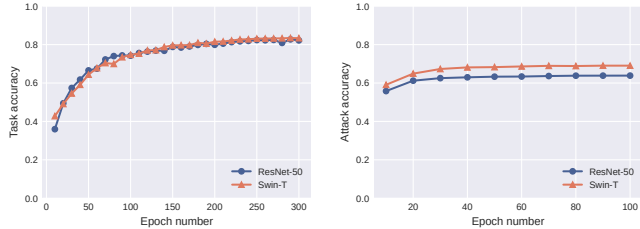
Victim Models. To ensure fair comparisons, we evaluate the performances of CNNs and Transformers with similar parameter sizes. For membership inference and attribute inference attacks, we select two groups of models based on their parameter sizes. These groups include ResNet-50, and ResNet-101 as CNN-based models, and Swin-T, and Swin-S as Transformer-based models. We train these models to reach more than 0.99 training accuracy.

Attack Models. For membership inference attacks, we employ a three-layer MLP model to infer membership information. Attribute inference attacks utilize a two-layer MLP model to uncover learned representations and potentially infer sensitive information. In gradient inversion attacks, we optimize input and generated gradients to reconstruct the original data, revealing private information.

Evaluation Metrics. We evaluate the performance of different attacks using specific metrics. For membership inference attacks, we consider attack accuracy (\uparrow), ROC curve (\uparrow), AUC (\uparrow), and TPR at low FPR (\uparrow). For attribute inference attacks, we assess effectiveness using attack accuracy (\uparrow) and macro-F1 score (\uparrow). Regarding gradient inversion attacks, we use multiple metrics to evaluate the quality of reconstruction results. These metrics include mean square error (MSE \downarrow), peak signal-to-noise ratio (PSNR \uparrow), learned perceptual image patch similarity (LPIPS \downarrow) [69], and structural similarity (SSIM \uparrow) [60]. Note that " \uparrow " means the higher metric corresponds to the higher attack performance, while \downarrow means the

Table 2: Results for network-based membership inference attacks.

	CIFAR10		CIFAR100	
	Task acc \uparrow	Attack acc \uparrow	Task acc \uparrow	Attack acc \uparrow
ResNet-50	0.8220 \pm 0.0023	0.6385 \pm 0.0078	0.5288 \pm 0.0083	0.8735 \pm 0.0029
Swin-T	0.8335 \pm 0.0042	0.6904 \pm 0.0052	0.5632 \pm 0.0056	0.9340 \pm 0.0030
ResNet-101	0.8301 \pm 0.0037	0.6317 \pm 0.0063	0.5313 \pm 0.0074	0.8607 \pm 0.0034
Swin-S	0.8258 \pm 0.0039	0.6405 \pm 0.0075	0.5665 \pm 0.0059	0.9357 \pm 0.0039



(a) Performance of victim models on CIFAR10 (b) Performance of privacy attack on CIFAR10

Figure 1: The performance of membership inference attacks against ResNet-50 and Swin-T on CIFAR10 under different numbers of epochs.

lower metric leads to the higher attack performance.

Training Settings for Privacy Attacks. Table 1 illustrates the training configurations for membership inference attacks, attribute inference attacks and gradient inversion attacks.

4.2 Evaluation on Membership Inference Attacks

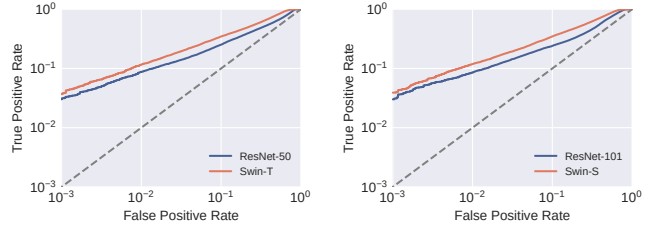
The results presented in Table 2 offer the performance of network-based membership inference attacks on CIFAR10 and CIFAR100 datasets. The task accuracy scores of the victim models on CIFAR10, which are approximately 0.82 for both CNNs and Transformers, indicate that these models exhibit competitive task performance with similar overfitting levels. Notably, the attack accuracy on CIFAR10 reveals that Transformers exhibit more privacy leakage compared to CNN models within each group. Similar findings are observed on CIFAR100, suggesting that Transformers consistently exhibit higher vulnerability to membership inference attacks compared to CNN models.

It is worth mentioning that the dataset used in this study is divided into four equally sized subsets for training and testing the victim and attack models. Consequently, the task accuracy of the victim models on CIFAR10 and CIFAR100 might be lower than expected in a standard CIFAR10 or CIFAR100 classification task. This does not affect the performance of the attacks and this phenomenon has been acknowledged in prior research [4, 17, 25, 47]. This also applies to later experimental results.

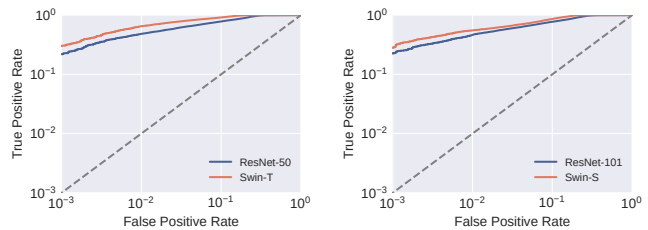
Figure 1 illustrates the task accuracy and attack accuracy of

Table 3: Results of likelihood-based membership inference attacks.

		Task acc \uparrow	AUC \uparrow	TPR@0.1%FPR \uparrow	Attack acc \uparrow
		CIFAR10	ResNet-50	0.8716 \pm 0.0035	0.6446 \pm 0.0276
	Swin-T	0.8630 \pm 0.0017	0.7384 \pm 0.0029	3.68% \pm 0.33%	0.6553 \pm 0.0027
	ResNet-101	0.8708 \pm 0.0043	0.6671 \pm 0.0107	3.33% \pm 0.41%	0.6090 \pm 0.0079
	Swin-S	0.8636 \pm 0.0036	0.7392 \pm 0.0054	3.75% \pm 0.37%	0.6576 \pm 0.0045
CIFAR100	ResNet-50	0.5632 \pm 0.0032	0.9431 \pm 0.0005	23.75% \pm 2.09%	0.8524 \pm 0.0009
	Swin-T	0.6001 \pm 0.0033	0.9756 \pm 0.0003	28.52% \pm 1.54%	0.9112 \pm 0.0010
	ResNet-101	0.5654 \pm 0.0042	0.9379 \pm 0.0021	21.25% \pm 1.55%	0.8484 \pm 0.0036
	Swin-S	0.5900 \pm 0.0029	0.9639 \pm 0.0006	31.02% \pm 1.74%	0.8978 \pm 0.0014



(a) ResNet-50 vs Swin-T on CIFAR10 (b) ResNet-101 vs Swin-S on CIFAR10



(c) ResNet-50 vs Swin-T on CIFAR100 (d) ResNet-101 vs Swin-S on CIFAR100

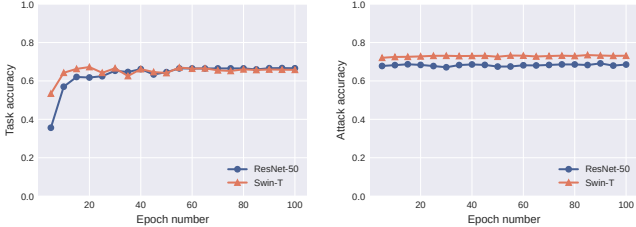
Figure 2: ROC curves for membership inference attacks on CIFAR10 and CIFAR100. Comparisons between CNNs and Transformers.

ResNet-50 and Swin-T across multiple epochs on CIFAR10. The task accuracy of ResNet-50 starts relatively low but exhibits a rapid increase over time. Eventually, both ResNet-50 and Swin-T reach task accuracy scores of approximately 0.82. Regarding attack accuracy, the plot demonstrates that the attack on Swin-T consistently outperforms the attack on ResNet-50.

Table 3 displays the outcomes of likelihood-based membership inference attacks on CIFAR10 and CIFAR100. The table includes task accuracy and attack performance like the evaluation for network-based attacks. To assess attack performance more comprehensively, we adopt the methodology proposed in [4] and incorporate additional metrics such as AUC, TPR@0.1%FPR, besides attack accuracy. The victim models achieve task accuracy scores of approximately 0.86 on CIFAR10 and 0.56 on CIFAR100. Consistently, the attack performance metrics highlight that Transformers are more vulnerable to membership inference attacks compared to CNNs

Table 4: Results of attribute inference attacks on CelebA.

	Task acc \uparrow	Attack acc \uparrow	Macro F1 \uparrow
ResNet-50	0.6666 \pm 0.0020	0.6854 \pm 0.0015	0.3753 \pm 0.0012
Swin-T	0.6587 \pm 0.0023	0.7312 \pm 0.0014	0.5530 \pm 0.0019
ResNet-101	0.6431 \pm 0.0029	0.6291 \pm 0.0023	0.4262 \pm 0.0009
Swin-S	0.6569 \pm 0.0024	0.7369 \pm 0.0036	0.5536 \pm 0.0015



(a) Performance of victim models on CelebA (b) Performance of privacy attack on CelebA

Figure 3: The performance of attribute inference attacks against ResNet-50 and Swin-T on CelebA under different numbers of epochs.

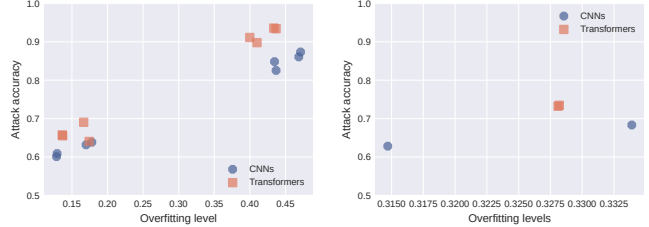
in terms of any attack metric. We also present the attack performance through ROC curves in Figure 2. These curves demonstrate that Transformers yield higher ROC curves, signifying their better attack performance.

The privacy leakage varies on different models and datasets. Similar to [46, 48], we analyze the overfitting levels of victims models in Figure 4a. The overfitting level indicates the accuracy difference of a model between its training and inference. Figure 4a illustrates the results of Transformers and CNNs in CIFAR10 and CIFAR100. We conclude that a more overfitted model comes with higher membership inference attack accuracy. More importantly, at the same overfitting level, Transformers always suffer from higher attack accuracy.

In conclusion, the results strongly suggest that Transformers are more susceptible to network-based and likelihood-based membership inference attacks compared to CNNs. Transformers consistently demonstrate higher vulnerability to membership inference attacks across various metrics.

4.3 Evaluation on Attribute Inference Attacks

Table 4 presents the results of attribute inference attacks on CelebA. Similarly to membership inference attacks, we categorize CNN and Transformer models into two groups based on their parameter sizes. The table shows that within each group, CNNs and Transformers achieve similar task accuracy scores, approximately 0.65. However, when considering the attack accuracy and Macro F1 score, Transformers consistently outperform CNNs. The results from attribute inference attacks align with our previous findings from membership inference attacks, emphasizing the increased vulnerability of



(a) Membership inference (b) Attribute inference

Figure 4: The performance of privacy attacks against both CNNs and Transformers with various models and datasets under different overfitting levels.

Table 5: The results of gradient inversion attacks on CNNs and Transformers on CIFAR10.

	MSE \downarrow	PSNR \uparrow	LPIPS \downarrow	SSIM \uparrow
ResNet-50	1.3308 \pm 0.6507	11.30 \pm 2.24	0.1143 \pm 0.0403	0.0946 \pm 0.0989
Swin-T	0.0069 \pm 0.0071	36.24 \pm 5.21	0.0012 \pm 0.0016	0.9892 \pm 0.0118
ResNet-101	1.2557 \pm 0.6829	11.58 \pm 2.16	0.1461 \pm 0.1012	0.0784 \pm 0.0675
Swin-S	0.0063 \pm 0.0083	37.85 \pm 6.15	0.0016 \pm 0.0028	0.9878 \pm 0.0128

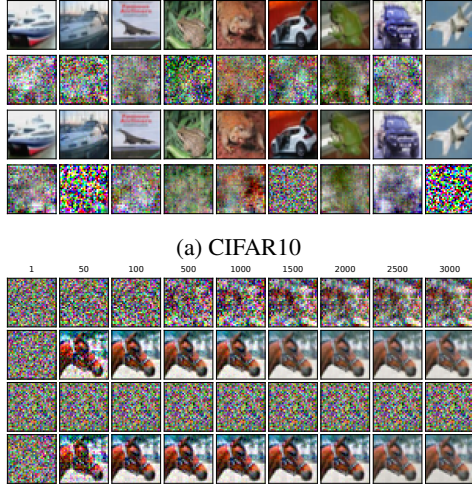
Transformer models to privacy attacks.

Figure 3 presents the performance of task accuracy and attack accuracy in attribute inference attacks using ResNet-50 and Swin-T on CelebA over 100 epochs. Figure 3a shows that although ResNet-50 and Swin-T models start with different task accuracy scores, both models gradually converge to similar task accuracy scores of around 0.65. However, when we examine the attack accuracy in Figure 3b, the attack accuracy on Swin-T consistently outperforms that on ResNet-50 throughout the 100 epochs. This reveals that Transformers like Swin-T are more vulnerable to attribute inference attacks than ResNet-50 from the start of the attack training to the end.

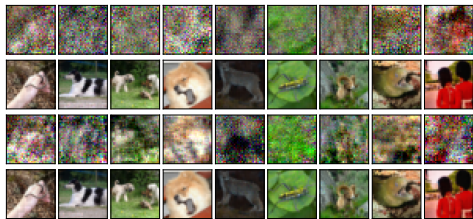
We further analyze the relationship between the attack performance and the overfitting levels of victim models in Figure 4b. We have made a similar discovery to the previous evaluation: Transformers suffer from higher attack accuracy than CNNs when the victim models are at the same overfitting level.

4.4 Evaluation on Gradient Inversion Attacks

Table 5 presents the results of gradient inversion attacks on CNNs and Transformers using CIFAR10. Similar to our previous evaluations, we still compare these two model architectures in groups. The attacks are evaluated by multiple metrics, which measure reconstruction results between ground truth images and reconstruction images. The table clearly shows that the attacks on Transformers outperform the attacks on CNNs by a significant margin. Figure 5a provides examples of the attack outputs, highlighting the difference between CNNs and Transformers. The attacks on CNNs fail to generate high-quality reconstruction images, whereas the attacks on



(b) CIFAR10 with different iteration numbers (i.e. 1, 50, 100, 500, 1000, 1500, 2000, 2500, 3000).



(c) ImageNet1K.

Figure 5: The performance of gradient inversion attacks on CNNs and Transformers. From the top row to the bottom in each subfigure are ResNet-50, Swin-T, ResNet-101, and Swin-S.

Transformers produce remarkably accurate reconstructions that closely resemble the originals.

Figure 5b provides the reconstruction results of the gradient inversion attacks over multiple iterations. It demonstrates the transformation of a raw dummy image towards a reconstruction that closely resembles the original image as the attack training continues. The reconstruction results reveal the varying degrees of success achieved by the attacks on different models. In the case of ResNet-50, the reconstructed image shows limited resemblance to the original image. When attacking ResNet-101, the reconstruction result fails to capture any meaningful information. On the other hand, when targeting Transformers such as Swin-T and Swin-S, the attacks yield highly accurate reconstruction results since early iterations.

In the evaluation of gradient inversion attacks on ImageNet1K, we still compare the performance of ResNet-50, ResNet-101, Swin-T, and Swin-S models. Randomly selected images from ImageNet1K are used to generate reconstruction results, shown in Figure 5c. Similar to the previous experiments on CIFAR10, the attacks on ResNet variants have

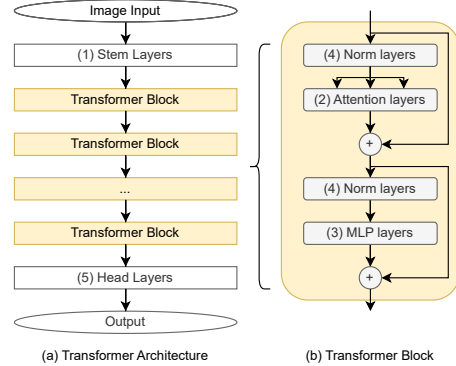


Figure 6: An illustration of a Vision Transformer architecture and the modules we focus on evaluating. Numbers (1) - (5) denote the modules we evaluate in gradient inversion attacks. (a): The whole model architecture. (b): Detailed architecture of each Transformer block.

limited success in reconstructing the original images. In contrast, the attacks on Transformer models (Swin-T and Swin-S) yield significantly better reconstruction results.

These findings highlight the higher vulnerability of Transformers to gradient inversion attacks compared to CNNs. This raises questions about specific architectural features in Transformers that contribute to their increased vulnerability to privacy attacks.

5 Which Architectural Features Can Lead to Higher Privacy Leakage?

In this section, we answer the fourth research question. We delve into analyzing architectural features that can potentially lead to privacy leakage. Through a comprehensive analysis, we first examine the impact of partitioning a transformer model on privacy vulnerabilities. Then we investigate the influence of various micro designs on model privacy and further conduct an ablation study on these micro designs.

5.1 Segmenting a Transformer Model to Analyze the Privacy Leakage

One of the key distinctions between a CNN and a Transformer lies in the design of their respective blocks. In this section, we focus on segmenting a Transformer-based model and assessing the potential influence of specific layers on privacy leakage. As there are only prediction results and model representations from membership inference attacks and attribute inference attacks, it is difficult to evaluate some specific layers using these attacks. However, gradient inversion attacks offer a more precise means of evaluation, as they require a comprehensive list of gradients from each layer of the victim model.

Table 6: The performance of gradient inversion attacks when segmenting ViT-B to make a selection of gradients.

Layers	Number of layers	MSE ↓	PSNR ↑
All layers	152	0.0007 ± 0.0003	43.70 ± 1.84
Stem layers	4	0.0000 ± 0.0000	67.43 ± 5.03
Attention layers	48	0.0020 ± 0.0009	39.61 ± 2.76
MLP layers	48	0.0036 ± 0.0016	36.98 ± 2.59
Norm layers	48	0.0040 ± 0.0018	36.57 ± 2.56
Head layers	4	0.2776 ± 0.2312	19.01 ± 3.89

In our analysis, we employ ViT-B as the victim model. This is because ViT models are one of the first Transformers in computer vision. Additionally, ViT models incorporate several common modules shared across various Transformer architectures. We utilize gradient inversion attacks as our chosen attack method. Rather than supplying all the gradients to the attacks, we selectively provide specific gradients for evaluation purposes. The architecture of a Vision Transformer (an example of ViT-B) is depicted in Figure 6. To facilitate our assessment, we divide the model into five distinct modules based on their layer designs. Subsequently, we evaluate the influence of gradients obtained from each module individually. If the attack using gradients from Module A yields a higher attack accuracy compared to the attack using gradients from Module B, it suggests that Module A is more likely to reveal more information about the data samples than Module B.

- Module 1: Stem layers. This module receives the input of the model and has patch embedding and position embedding layers.
- Module 2: Attention layers. They are in the Transformer block, and this module is the main reason why Transformers are different from CNNs.
- Module 3: MLP layers. They are also in the Transformer block.
- Module 4: Norm layers. They are located right before the attention layers and MLP layers. LayerNorm is often used as Norm layers in Transformers.
- Module 5: Head layers. They are the last few layers for producing the output of the model. A few fully connected layers could be used as head layers.

Table 6 presents the reconstruction results of gradient inversion attacks when only gradients from selected layers are utilized in the attacks. The "All layers" represents the default attack scenario, where gradients from all layers are employed. The stem layers contain the patch embedding and position embedding processes. These layers exhibit minimal changes in the output compared to the original image sample. As the stem layers comprise only four layers, they can be relatively easier to attack compared to other types of layers. Consequently, the attacks on the stem layers demonstrate excellent performance, and we will further assess stem layers in the next subsection.

Table 7: Attack performance on ConvNeXt-T compared with ResNet-50 and Swin-T. NN MIA for Network-based membership inference, GIA for gradient inversion.

		ResNet-50	ConvNeXt-T	Swin-T
NN MIA	Attack acc ↑	0.6385 ± 0.0078	0.7471 ± 0.0052	0.6904 ± 0.0052
GIA	MSE ↓	1.5096 ± 0.5538	0.0177 ± 0.0171	0.0069 ± 0.0071
	PSNR ↑	10.58 ± 1.87	31.88 ± 5.04	36.24 ± 5.21
	LPIPS ↓	0.1624 ± 0.0613	0.0032 ± 0.0055	0.0012 ± 0.0016
	SSIM ↑	0.0896 ± 0.0544	0.9666 ± 0.0451	0.9892 ± 0.0118

Among the attacks conducted with the remaining selected layers, the attack that demonstrates the best performance is the one utilizing "attention layers." This attack achieves an MSE of 0.0020 and a PSNR of 39.61. These results indicate that the attention layers are more susceptible to attacks, suggesting that they potentially leak more information about the data samples.

5.2 Impact of Other Micro Designs on Privacy

In the previous subsection, we established that attention layers within Transformers can contribute to privacy leakage. However, it's important to recognize that other micro designs within Transformers may also have an impact on privacy vulnerabilities. One example is ConvNeXt [34], a convolutional neural network that incorporates multiple schemes from the Transformer model, similar to the Swin Transformer. ConvNeXt-T, ResNet-50, and Swin-T all share a similar parameter size, with ConvNeXt-T having approximately 27.83 million parameters. This allows for directly comparing the attack performance between ConvNeXt-T and the other two models. When ConvNeXt-T is tested on CIFAR10 using the same attack settings, it achieves a task accuracy of 0.8258. This indicates that we can compare the attack performance of ConvNeXt-T with ResNet-50 and Swin-T. The results presented in Table 7 further confirm the high attack performance on ConvNeXt-T. These findings suggest that ConvNeXt-T and Swin-T exhibit vulnerability to various attacks at a similar level.

The difference between ConvNeXt and the Swin Transformer lies in the attention module. This presents us with a valuable opportunity to explore and investigate the privacy implications of various micro designs in model architectures beyond just the attention layers. By studying the impact of different micro designs, we can gain deeper insights into the specific architectural features that may pose privacy risks.

We continue with utilizing gradient inversion attacks as a tool for further examination. Following the design process outlined in [34], we have made several adjustments based on our own analysis. Since ConvNeXt is constructed incrementally from ResNet, we meticulously scrutinized each model architecture throughout the process to investigate the steps that contribute most significantly to privacy leakage. We focus on ResNet-50 and ConvNeXt-T models and conduct tests

on a total of 14 model architectures using randomly selected samples from the CIFAR10.

The analysis involves a 14-step process, wherein we begin by modifying the overall architecture (Steps 1 to 4) based on ResNet-50. Subsequently, we focus on aligning the bottleneck design (Steps 5 to 7) and refining the stem layer design in Step 8. Finally, we align the micro designs (Steps 9 to 14) to achieve ConvNeXt-T. This 14-step process, as outlined in [34], has been established as an optimal procedure for designing ConvNeXt. Leveraging this proven methodology, we utilize it to analyze the impact on privacy. By identifying the critical steps that contribute to privacy leakage, we can assess the influence of micro designs on the privacy of model architectures. This analysis provides valuable insights into understanding the specific stages or modifications that may pose risks to privacy. The 14 steps are outlined below:

1. **ResNet-50:** We begin our process with this model.
2. **Changing channel dimensions:** In ResNet-50, each stage uses different channel dimensions (i.e., (64, 128, 256, 512)). To align with ConvNeXt-T, we modify these dimensions to (96, 192, 384, 768).
3. **Changing the stage compute ratio:** ResNet employs a multi-stage design that modifies channel dimensions. ResNet-50 has a stage compute ratio of (3, 4, 6, 3), while ConvNeXt and Swin Transformers adopt (3, 3, 9, 3). We follow this adjustment in this step.
4. **Applying "Patchify":** Vision transformers process input images by sliding them into patches. Here, we replace the stem convolutional layers with a kernel size of (4×4) and a stride of 4.
5. **Applying "ResNeXtify":** ResNeXt [62] introduced grouped convolution, reducing parameter size while maintaining performance. We utilize depth-wise convolution, which employs the same number of groups and channels.
6. **Using the inverted bottleneck:** The inverted bottleneck design is widely employed in models like MobileNet, ConvNeXt, and Swin Transformers. We incorporate this step into our process.
7. **Enlarging kernel sizes:** To align the parameters with ConvNeXt, we adopt a larger kernel size of (7×7) instead of (3×3).
8. **Forming the new stem layers:** In this step, we remove the activation layer and the maxpool layer, which were originally part of ResNet.
9. **Changing ReLU to GELU:** The Gaussian Error Linear Unit (GELU) [19] is a variant of ReLU commonly used in Transformers. We introduce this change to the model.
10. **Removing some activation layers:** Transformer blocks typically have fewer activation layers. Here, we retain only one activation layer within the block.

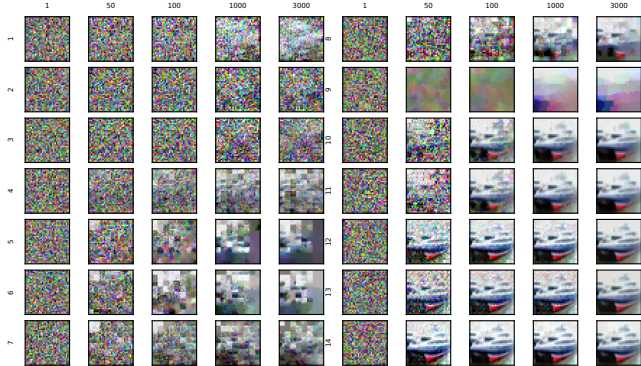


Figure 7: The performance of gradient inversion attacks on each architecture changing from ResNet-50 to ConvNeXt-T with several selected iterations (i.e. 1, 50, 100, 1000, 3000). Model architectures from 14 steps are shown.

11. **Removing some normalization layers:** We reduce the number of BatchNorm (BN) layers within the block to one.
12. **Changing BN to LN:** Inspired by the prevalent use of LayerNorm (LN) layers [1] in Transformers, we replace the BN layers in our model with LN layers. And we also enable bias parameters for all convolutional layers in this step.
13. **Separating downsampling layers:** We move the downsampling layers between stages, introducing an LN layer to ensure stability during training.
14. **Final touches to reach ConvNeXt-T:** We incorporate Stochastic Depth [22] and Layer Scale [57] in the final stage to complete the ConvNeXt-T model.

Please refer to Appendix B for more detailed architecture specifications.

Figure 7 and Table 8 show the performance of gradient inversion attacks on each model architecture. The observed trend indicates that the reconstruction results are getting better with the architecture changing.

Figure 7 provides qualitative results of the attacks. During the initial stages (Steps 1 to 3), the attacks struggle to reconstruct proper images. In the middle stages, some information starts to emerge in the reconstruction results but to a limited extent. The reconstruction results improve in the later stages (After Step 10). At last, using ConvNeXt-T, which is step 14, the attacks achieve a good attack performance.

Table 8 presents more information on the performance of gradient inversion attacks. There are three significant increases in attack performance when the architecture changes step by step: the first one occurs when "Patchify" is applied to stem layers; the second one occurs when some activation layers are removed; the third one happens when changing BN to LN. These findings suggest that these specific architectural

Table 8: The results of gradient inversion attacks on model architectures from 14 steps. Some significant changes in results are marked in bold.

Steps	Task acc \uparrow	MSE \downarrow	PSNR \uparrow	LPIPS \downarrow	SSIM \uparrow
1. ResNet-50	0.8220 \pm 0.0039	1.5096 \pm 0.5538	10.58 \pm 1.87	0.1624 \pm 0.0613	0.0896 \pm 0.0544
2. Channel dim	0.8240 \pm 0.0072	1.4706 \pm 0.5710	10.74 \pm 1.97	0.1724 \pm 0.0616	0.0826 \pm 0.0405
3. Stage ratio	0.8282 \pm 0.0040	1.5286 \pm 0.5246	10.56 \pm 2.05	0.1834 \pm 0.0581	0.0731 \pm 0.0613
4. Patchify	0.8293 \pm 0.0061	0.9011 \pm 0.4376	12.97 \pm 2.10	0.0867 \pm 0.0436	0.1727 \pm 0.0794
5. ResNeXtify	0.8397 \pm 0.0033	1.2415 \pm 0.6934	11.86 \pm 2.77	0.1066 \pm 0.0391	0.1334 \pm 0.0950
6. Inv bottleneck	0.8407 \pm 0.0058	1.1123 \pm 0.4994	12.06 \pm 2.19	0.0989 \pm 0.0290	0.1429 \pm 0.0844
7. Kernel sizes	0.8432 \pm 0.0052	0.8206 \pm 0.3543	13.40 \pm 2.30	0.0821 \pm 0.0355	0.2353 \pm 0.0766
8. New stem	0.8459 \pm 0.0043	0.5684 \pm 0.3564	15.43 \pm 3.01	0.0752 \pm 0.0381	0.4924 \pm 0.1205
9. ReLU to GELU	0.8436 \pm 0.0027	1.0540 \pm 0.5075	12.42 \pm 2.61	0.2422 \pm 0.0904	0.1746 \pm 0.1166
10. Removing Act	0.8480 \pm 0.0064	0.0215 \pm 0.0150	29.93 \pm 3.58	0.0049 \pm 0.0026	0.9562 \pm 0.0224
11. Removing BN	0.8491 \pm 0.0059	0.0198 \pm 0.0139	30.57 \pm 4.12	0.0045 \pm 0.0032	0.9605 \pm 0.0232
12. BN to LN	0.8501 \pm 0.0031	0.0049 \pm 0.0044	36.86 \pm 3.96	0.0005 \pm 0.0003	0.9927 \pm 0.0064
13. Sep downsamp	0.8553 \pm 0.0070	0.0121 \pm 0.0171	33.79 \pm 4.69	0.0011 \pm 0.0008	0.9859 \pm 0.0151
14. ConvNeXt	0.8523 \pm 0.0064	0.0177 \pm 0.0171	31.88 \pm 5.04	0.0032 \pm 0.0055	0.9666 \pm 0.0451

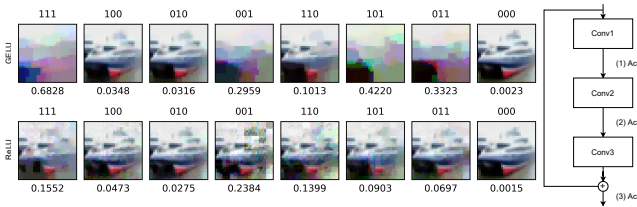


Figure 8: The performance of gradient inversion attacks on models with different positions of activation layers. The position of three activation layers is illustrated on the right, with two between convolutional layers and one after the addition operation. The three digits on the top of the subfigures show whether the activation layer on this position is added or not. The bottom of each subfigure provides MSE values for the attack on this model (i.e. models with GELU or ReLU).

changes play a crucial role in determining the vulnerability of the model to privacy attacks.

5.3 Ablation Study on Micro Designs

Ablation study on the design of activation layers. One of the differences between a Transformer block and a ResNet block is that a Transformer block has fewer activation layers. Leaving fewer activation layers in the model boosts the attack performance. As illustrated in Figure 8, when different activation layers are removed, there is a noticeable improvement in the attack performance. Particularly, the removal of the third activation layer, located after the skip connection of the ResNet block, results in a significant enhancement in attack accuracy. This observation suggests that the presence of this activation layer introduces a non-linear process that reduces the amount of information available for the attack, thus making it harder to reconstruct the original input. By removing this layer, the attack performance is improved. The analysis also indicates that changing ReLU to GELU does not contribute to improving the attack performance. Instead, the

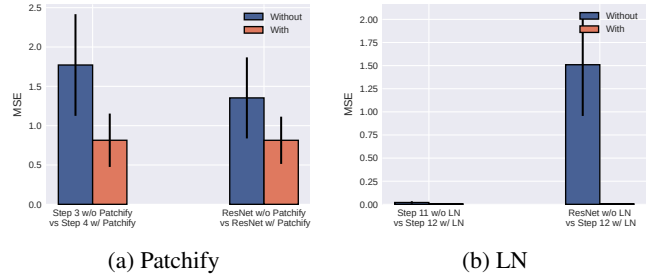


Figure 9: The performance of gradient inversion attacks on model architectures with or without some features.

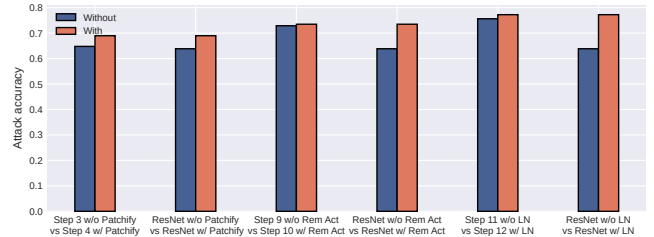


Figure 10: The performance of membership inference attacks on model architectures with or without some features.

best reconstruction results are achieved when all activation layers are removed from the model architecture.

Ablation study on the design of stem layers and LN layers. The additional analysis presented in Figure 9 highlights two more features that appear to have an impact on model privacy leakage. Firstly, Figure 9a demonstrates that the utilization of "Patchify" reduces reconstruction MSE results. As this process involves modifications to the stem layers, we believe that these stem layers are crucial for privacy attacks. Secondly, Figure 9b illustrates that changing BN to LN results in improved reconstruction results. This suggests that incorporating LN also contributes to the model's privacy leakage. These findings emphasize the significance of stem layers and LN layers on model privacy leakage.

Ablation study on micro designs for membership inference attacks. Figure 10 shows the impact of three micro designs on membership inference attacks. Just like previous studies, adding these designs can increase privacy leakage in membership inference attacks as well.

6 Discussion

In the previous sections, we discovered that four design components in Transformers could result in privacy leakage: attention modules, activation layers, stem layers, and LN layers. In this section, we would like to provide a more in-depth discussion of these modules.

6.1 The Impact of Attention Modules

The receptive field of a model refers to the information received within a specified range by a neuron in a model layer. In a fully connected neural network, each neuron receives input from the elements of the entire input sample. Due to the convolution operation, the neuron in a convolutional network receives input limited to its receptive field. The range of the receptive field is defined by the convolution templates in CNNs. This design allows CNNs to capture local patterns in the input data efficiently. The receptive field has a theoretical limit. Some researchers have demonstrated that the effective receptive field (i.e. the effective area in the receptive field) is actually smaller than the theoretical receptive field [38]. From a privacy perspective, a CNN model could only reveal part of sensitive information from the input sample due to the design of localized convolution templates.

Transformers employ the multi-head self-attention mechanism, also known as attention modules. The input sample is taken as a sequence of flattened 2D patches. The attention module receives the input sequence and generates its representation of the sequence by mapping the query and the key-value pairs to the output. Transformers tend to have much larger receptive fields than CNNs due to the fact that their attention module is computed with the entire input sequence [10,59]. In terms of privacy, a Transformer model is able to extract more sensitive information than a CNN model because of its wide-angle receptive field. Hence, Transformers are more prone to attacks than CNNs, as demonstrated by our evaluation based on three popular privacy attacks.

6.2 The Impact of Micro Designs

There are micro-design components with the potential to leak sensitive data from input samples. Activation layers such as ReLU and GELU add a layer of complexity to the model by making it a non-linear function. Removing some activation layers simplifies the logic of attacks. Stem layers receive an input sample and perform some preliminary processing. As the representation after the stem layers remains similar to the

original input image, there is a high possibility of extracting private information because of the design of the stem layers. Changing BN to LN is also likely to aid the attack process and allow the adversary to achieve higher attack performance.

6.3 The Impact of Overfitting

Previous work claimed that privacy attacks are mostly caused by the undesirable overfitting issue in deep learning models [32,48]. Overfitting normally occurs when a model performs well on the training data, but poorly on the validation data. The overfitting issue tends to become severe on an over-trained model with a large number of parameters. Deep learning models are exposed to privacy threats due to the overfitting effect. In our work, we find that model architectures have impacts on the performance of privacy attacks, which can *not* be attributed solely to the overfitting effect. Indeed, our experiments validate that the variation in performance is due to the difference in model architectures. For models with the same level of parameter sizes, Transformers tend to be more vulnerable to privacy attacks than CNNs. More importantly, for models with the same overfitting level, our conclusion still holds that Transformers are more vulnerable to privacy attacks than CNNs. We have then identified some architectural features that could be responsible for privacy leakage.

6.4 Potential (Incorrect) Explanations for the Vulnerability of Different Models Against Privacy Attacks

Here we outline several alternative potential explanations for our experimental results.

- The attacks on Transformers are more effective than those on CNNs. Is it due to statistical noise? To mitigate this concern, we have conducted multiple runs for each experiment setting and calculated the mean and standard deviation scores of our results. We have done around 100 different experiment settings, 1400 experiments, 1700 training models, and 1200 training hours, which averages out the impact of statistical noise.
- Is it due to the overfitting of the victim models? To account for this, we meticulously compare the attacks on CNNs and Transformers when their victim models are trained on the same level of overfitting. By doing so, we minimize the influence of overfitting for a fair assessment.
- Is it due to the immature training of the victim models? In order to conduct our experiments, it was necessary to split the dataset into multiple subsets for both victim models and shadow models. Consequently, it is reasonable to expect relatively low accuracy on the victim models for CIFAR10, CIFAR100, and CelebA (compared to

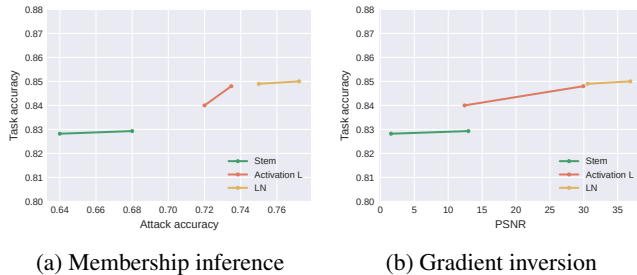


Figure 11: The impact of the performance of privacy attacks when model components change.

models for a full dataset). This aligns with the findings of numerous privacy attack literature, which have reported similar results. [4, 17, 32].

- Is it due to other training factors? We ensure that the training recipes for each victim model remained consistent across all comparisons. Consequently, we can confidently exclude other training factors.

After eliminating these potential explanations, we believe that the cause of our experimental results is still due to several architectural features mentioned in the previous section.

7 How to Exploit the Privacy Impact of Model Components?

7.1 Modifying Model Components as a Defense Mechanism

Based on our discoveries in previous sections, we propose to explore the modification of model components as a defense mechanism against privacy attacks. We aim to achieve a trade-off between utility and privacy. In Figure 11, we demonstrate the influence of certain micro-design changes on the efficacy of privacy attacks. In each line of the figures, the left and right points represent the results without and with the micro design modifications, respectively. Notably, we observe that the task accuracy is minimally impacted in each test, indicating that the proposed defense measures do not significantly compromise the overall performance of the model. However, we can observe a decreased effectiveness of membership inference attacks and gradient inversion attacks.

These findings suggest that the proposed micro-design modifications can serve as effective countermeasures against privacy attacks, while the task accuracy remains almost intact.

7.2 Adding Perturbations as a Defense Mechanism

The privacy leakage issue observed in Transformers highlights the need for an enhanced privacy treatment compared

to CNNs. Specifically, when employing perturbation as a defense mechanism, such as incorporating differential privacy noises into the model parameters, it is better to increase the level of noise specifically for Transformers and Transformer-like models.

Another approach to consider is a layer-wise perturbation defense mechanism, where noises are added to selected layers only. In this scenario, it would be interesting to introduce additional noises to the layers that are more susceptible to privacy leakages, such as activation layers, stem layers, LN layers, and attention modules. By paying special attention to these "privacy-leakage" layers, the total level of perturbation could be lowered while achieving satisfactory privacy protection. This method of uneven noise perturbation across various Transformer modules will be a part of our future work.

8 Conclusion

In this study, for the first time, we perform privacy risk analysis on model architectures, especially CNNs and Transformers. We have conducted a comparison of three prominent privacy attacks, i.e., membership inference attacks, attribute inference attacks, and gradient inversion attacks. We discover that Transformers tend to be more vulnerable to privacy attacks than CNNs. As a result, many Transformers-inspired CNN designs, such as ConvNeXt, are also susceptible to privacy threats. A number of Transformers' features, including the design of activation layers, the design of stem layers, the design of LN layers, and the attention modules, may have incurred high privacy risks.

It is still challenging to establish accurate and theoretical explanations for why certain architectural features are critical to privacy preservation. We believe that these analyses require further experimental campaigns, and we intend to study this in our future work.

References

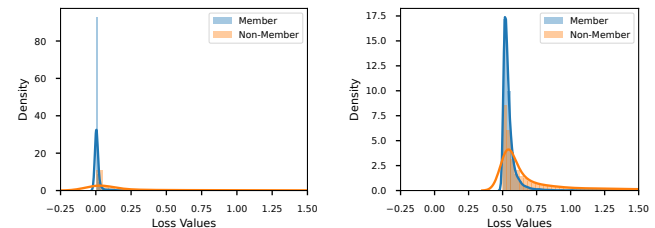
- [1] Jimmy Lei Ba, Jamie Ryan Kiros, and Geoffrey E. Hinton. Layer Normalization. *arXiv preprint arXiv:1607.06450*, 2016.
- [2] Yutong Bai, Jieru Mei, Alan L Yuille, and Cihang Xie. Are Transformers more robust than CNNs? In *Advances in Neural Information Processing Systems*, volume 34, pages 26831–26843, 2021.
- [3] Tom Brown, Benjamin Mann, Nick Ryder, Melanie Subbiah, Jared D Kaplan, Prafulla Dhariwal, et al. Language Models are Few-Shot Learners. In *Advances in Neural Information Processing Systems*, volume 33, pages 1877–1901, 2020.
- [4] Nicholas Carlini, Steve Chien, Milad Nasr, Shuang Song, Andreas Terzis, and Florian Tramèr. Membership Inference Attacks From First Principles. In *2022 IEEE Symposium on Security and Privacy (SP)*, pages 1897–1914, 2022.
- [5] Dingfan Chen, Ning Yu, Yang Zhang, and Mario Fritz. GAN-Leaks: A Taxonomy of Membership Inference Attacks against

- Generative Models. In *Proceedings of the 2020 ACM SIGSAC Conference on Computer and Communications Security*, pages 343–362, 2020.
- [6] Min Chen, Zhikun Zhang, Tianhao Wang, Michael Backes, Mathias Humbert, and Yang Zhang. When Machine Unlearning Jeopardizes Privacy. In *Proceedings of the 2021 ACM SIGSAC Conference on Computer and Communications Security*, pages 896–911, 2021.
- [7] Christopher A. Choquette-Choo, Florian Tramer, Nicholas Carlini, and Nicolas Papernot. Label-Only Membership Inference Attacks. In *International Conference on Machine Learning*, pages 1964–1974, 2021.
- [8] Jia Deng, Wei Dong, Richard Socher, Li-Jia Li, Kai Li, and Li Fei-Fei. ImageNet: A large-scale hierarchical image database. In *2009 IEEE Conference on Computer Vision and Pattern Recognition*, pages 248–255, 2009.
- [9] Jacob Devlin, Ming-Wei Chang, Kenton Lee, and Kristina Toutanova. BERT: Pre-training of Deep Bidirectional Transformers for Language Understanding. In *NAACL-HLT*, pages 4171–4186, 2019.
- [10] Alexey Dosovitskiy, Lucas Beyer, Alexander Kolesnikov, Dirk Weissenborn, Xiaohua Zhai, Thomas Unterthiner, et al. An Image is Worth 16x16 Words: Transformers for Image Recognition at Scale. In *International Conference on Learning Representations*, 2021.
- [11] Vasisht Duddu and Antoine Boutet. Inferring Sensitive Attributes from Model Explanations. *arXiv preprint arXiv:2208.09967*, 2022.
- [12] Matt Fredrikson, Somesh Jha, and Thomas Ristenpart. Model Inversion Attacks that Exploit Confidence Information and Basic Countermeasures. In *Proceedings of the 22nd ACM SIGSAC Conference on Computer and Communications Security*, pages 1322–1333, 2015.
- [13] Jonas Geiping, Hartmut Bauermeister, Hannah Dröge, and Michael Moeller. Inverting Gradients - How easy is it to break privacy in federated learning? *Advances in Neural Information Processing Systems*, 33:16937–16947, 2020.
- [14] Ali Hatamizadeh, Hongxu Yin, Holger R. Roth, Wenqi Li, Jan Kautz, Daguang Xu, and Pavlo Molchanov. GradViT: Gradient Inversion of Vision Transformers. In *Proceedings of the IEEE/CVF Conference on Computer Vision and Pattern Recognition*, pages 10021–10030, 2022.
- [15] Jamie Hayes, Luca Melis, George Danezis, and Emiliano De Cristofaro. LOGAN: Membership Inference Attacks Against Generative Models. *Proceedings on Privacy Enhancing Technologies*, 2019:133–152, 2019.
- [16] Kaiming He, Xiangyu Zhang, Shaoqing Ren, and Jian Sun. Deep Residual Learning for Image Recognition. In *2016 IEEE Conference on Computer Vision and Pattern Recognition (CVPR)*, pages 770–778, 2016.
- [17] Xinlei He and Yang Zhang. Quantifying and Mitigating Privacy Risks of Contrastive Learning. In *Proceedings of the 2021 ACM SIGSAC Conference on Computer and Communications Security*, pages 845–863, 2021.
- [18] Yang He, Shadi Rahimian, Bernt Schiele, and Mario Fritz. Segmentations-Leak: Membership Inference Attacks and Defenses in Semantic Image Segmentation. In *Computer Vision – ECCV 2020*, pages 519–535, 2020.
- [19] Dan Hendrycks and Kevin Gimpel. Gaussian Error Linear Units (GELUs). *arXiv preprint arXiv:1606.08415*, 2016.
- [20] Andrew Howard, Mark Sandler, Bo Chen, Weijun Wang, Liang-Chieh Chen, Mingxing Tan, et al. Searching for MobileNetV3. In *2019 IEEE/CVF International Conference on Computer Vision (ICCV)*, pages 1314–1324, 2019.
- [21] Hongsheng Hu, Zoran Salcic, Lichao Sun, Gillian Dobbie, Philip S. Yu, and Xuyun Zhang. Membership Inference Attacks on Machine Learning: A Survey. *ACM Computing Surveys*, 2022.
- [22] Gao Huang, Yu Sun, Zhuang Liu, Daniel Sedra, and Kilian Q. Weinberger. Deep Networks with Stochastic Depth. In *Computer Vision – ECCV 2016*, pages 646–661, 2016.
- [23] Bargav Jayaraman and David Evans. Are Attribute Inference Attacks Just Imputation? In *Proceedings of the 2022 ACM SIGSAC Conference on Computer and Communications Security*, pages 1569–1582, 2022.
- [24] Bargav Jayaraman, Lingxiao Wang, Katherine Knipmeyer, Quanquan Gu, and David Evans. Revisiting Membership Inference Under Realistic Assumptions. *Proceedings on Privacy Enhancing Technologies*, 2021:348–368, 2021.
- [25] Yigitcan Kaya and Tudor Dumitras. When Does Data Augmentation Help With Membership Inference Attacks? In *International Conference on Machine Learning*, pages 5345–5355, 2021.
- [26] A. Krizhevsky. Learning multiple layers of features from tiny images. 2009.
- [27] Alex Krizhevsky, Ilya Sutskever, and Geoffrey E Hinton. ImageNet Classification with Deep Convolutional Neural Networks. In *Advances in Neural Information Processing Systems*, volume 25, 2012.
- [28] Y. LeCun, B. Boser, J. S. Denker, D. Henderson, R. E. Howard, W. Hubbard, and L. D. Jackel. Backpropagation Applied to Handwritten Zip Code Recognition. *Neural Computation*, 1:541–551, 1989.
- [29] Zheng Li and Yang Zhang. Membership Leakage in Label-Only Exposures. In *ACM SIGSAC Conference on Computer and Communications Security (CCS 2021)*, 2021.
- [30] Zhuohang Li, Jiaxin Zhang, Luyang Liu, and Jian Liu. Auditing Privacy Defenses in Federated Learning via Generative Gradient Leakage. In *Proceedings of the IEEE/CVF Conference on Computer Vision and Pattern Recognition*, pages 10132–10142, 2022.
- [31] Bo Liu, Ming Ding, Sina Shaham, Wenny Rahayu, Farhad Farokhi, and Zihuai Lin. When Machine Learning Meets Privacy: A Survey and Outlook. *ACM Computing Surveys*, 54:31:1–31:36, 2021.
- [32] Yugeng Liu, Rui Wen, Xinlei He, Ahmed Salem, Zhikun Zhang, Michael Backes, Emiliano De Cristofaro, Mario Fritz, and Yang Zhang. ML-Doctor: Holistic Risk Assessment of Inference Attacks Against Machine Learning Models. In *31st USENIX Security Symposium (USENIX Security 22)*, 2022.

- [33] Ze Liu, Yutong Lin, Yue Cao, Han Hu, Yixuan Wei, Zheng Zhang, Stephen Lin, and Baining Guo. Swin Transformer: Hierarchical Vision Transformer using Shifted Windows. In *2021 IEEE/CVF International Conference on Computer Vision (ICCV)*, pages 9992–10002, 2021.
- [34] Zhuang Liu, Hanzi Mao, Chao-Yuan Wu, Christoph Feichtenhofer, Trevor Darrell, and Saining Xie. A ConvNet for the 2020s. In *2022 IEEE Conference on Computer Vision and Pattern Recognition (CVPR)*, 2022.
- [35] Ziwei Liu, Ping Luo, Xiaogang Wang, and Xiaoou Tang. Deep Learning Face Attributes in the Wild. In *2015 IEEE International Conference on Computer Vision (ICCV)*, pages 3730–3738, 2015.
- [36] Yunhui Long, Lei Wang, Diyue Bu, Vincent Bindschaedler, Xiaofeng Wang, Haixu Tang, Carl A. Gunter, and Kai Chen. A Pragmatic Approach to Membership Inferences on Machine Learning Models. In *2020 IEEE European Symposium on Security and Privacy (EuroS&P)*, pages 521–534, 2020.
- [37] Jiahao Lu, Xi Sheryl Zhang, Tianli Zhao, Xiangyu He, and Jian Cheng. APRIL: Finding the Achilles’ Heel on Privacy for Vision Transformers. In *Proceedings of the IEEE/CVF Conference on Computer Vision and Pattern Recognition*, pages 10051–10060, 2022.
- [38] Wenjie Luo, Yujia Li, Raquel Urtasun, and Richard Zemel. Understanding the Effective Receptive Field in Deep Convolutional Neural Networks. In *Advances in Neural Information Processing Systems*, volume 29, 2016.
- [39] Shagufta Mehnaz, Sayanton V. Dibbo, Ehsanul Kabir, Ninghui Li, and Elisa Bertino. Are Your Sensitive Attributes Private? Novel Model Inversion Attribute Inference Attacks on Classification Models. In *31st USENIX Security Symposium (USENIX Security 22)*, pages 4579–4596, 2022.
- [40] Luca Melis, Congzheng Song, Emiliano De Cristofaro, and Vitaly Shmatikov. Exploiting Unintended Feature Leakage in Collaborative Learning. In *2019 IEEE Symposium on Security and Privacy (SP)*, pages 691–706, 2019.
- [41] Milad Nasr, Reza Shokri, and Amir Houmansadr. Comprehensive Privacy Analysis of Deep Learning: Passive and Active White-box Inference Attacks against Centralized and Federated Learning. In *2019 IEEE Symposium on Security and Privacy (SP)*, pages 739–753, 2019.
- [42] Sayak Paul and Pin-Yu Chen. Vision Transformers Are Robust Learners. *Proceedings of the AAAI Conference on Artificial Intelligence*, 36:2071–2081, 2022.
- [43] Ilija Radosavovic, Raj Prateek Kosaraju, Ross Girshick, Kaiming He, and Piotr Dollar. Designing Network Design Spaces. In *Proceedings of the IEEE/CVF Conference on Computer Vision and Pattern Recognition*, pages 10428–10436, 2020.
- [44] Maithra Raghu, Thomas Unterthiner, Simon Kornblith, Chiyuan Zhang, and Alexey Dosovitskiy. Do Vision Transformers See Like Convolutional Neural Networks? In *Advances in Neural Information Processing Systems*, volume 34, pages 12116–12128, 2021.
- [45] Alexandre Sablayrolles, Matthijs Douze, Cordelia Schmid, Yann Ollivier, and Herve Jegou. White-box vs Black-box: Bayes Optimal Strategies for Membership Inference. In *International Conference on Machine Learning*, pages 5558–5567, 2019.
- [46] Ahmed Salem, Yang Zhang, Mathias Humbert, Pascal Berrang, Mario Fritz, and Michael Backes. ML-Leaks: Model and data independent membership inference attacks and defenses on machine learning models. In *26th Annual Network and Distributed System Security Symposium, NDSS 2019*, 2019.
- [47] Virat Shejwalkar and Amir Houmansadr. Membership Privacy for Machine Learning Models Through Knowledge Transfer. *Proceedings of the AAAI Conference on Artificial Intelligence*, 35:9549–9557, 2021.
- [48] Reza Shokri, Marco Stronati, Congzheng Song, and Vitaly Shmatikov. Membership Inference Attacks Against Machine Learning Models. In *2017 IEEE Symposium on Security and Privacy (SP)*, pages 3–18, 2017.
- [49] Karen Simonyan and Andrew Zisserman. Very Deep Convolutional Networks for Large-Scale Image Recognition. *arXiv preprint arXiv:1409.1556*, 2015.
- [50] Congzheng Song and Ananth Raghunathan. Information Leakage in Embedding Models. In *Proceedings of the 2020 ACM SIGSAC Conference on Computer and Communications Security*, pages 377–390, 2020.
- [51] Congzheng Song and Vitaly Shmatikov. Overlearning Reveals Sensitive Attributes. In *International Conference on Learning Representations*, 2020.
- [52] Liwei Song and Prateek Mittal. Systematic Evaluation of Privacy Risks of Machine Learning Models. In *30th USENIX Security Symposium (USENIX Security 21)*, pages 2615–2632, 2021.
- [53] Andreas Peter Steiner, Alexander Kolesnikov, Xiaohua Zhai, Ross Wightman, Jakob Uszkoreit, and Lucas Beyer. How to train your ViT? Data, augmentation, and regularization in vision transformers. *Transactions on Machine Learning Research*, 2022.
- [54] Christian Szegedy, Wei Liu, Yangqing Jia, Pierre Sermanet, Scott Reed, Dragomir Anguelov, Dumitru Erhan, Vincent Vanhoucke, and Andrew Rabinovich. Going deeper with convolutions. In *2015 IEEE Conference on Computer Vision and Pattern Recognition (CVPR)*, pages 1–9, 2015.
- [55] Christian Szegedy, Vincent Vanhoucke, Sergey Ioffe, Jon Shlens, and Zbigniew Wojna. Rethinking the Inception Architecture for Computer Vision. In *2016 IEEE Conference on Computer Vision and Pattern Recognition (CVPR)*, pages 2818–2826, 2016.
- [56] Hugo Touvron, Matthieu Cord, Matthijs Douze, Francisco Massa, Alexandre Sablayrolles, and Herve Jegou. Training data-efficient image transformers & distillation through attention. In *Proceedings of the 38th International Conference on Machine Learning*, pages 10347–10357, 2021.
- [57] Hugo Touvron, Matthieu Cord, Alexandre Sablayrolles, Gabriel Synnaeve, and Hervé Jégou. Going deeper with Image Transformers. In *2021 IEEE/CVF International Conference on Computer Vision (ICCV)*, pages 32–42, 2021.

- [58] Stacey Truex, Ling Liu, Mehmet Emre Gursoy, Lei Yu, and Wenqi Wei. Demystifying Membership Inference Attacks in Machine Learning as a Service. *IEEE Transactions on Services Computing*, pages 1–1, 2019.
- [59] Ashish Vaswani, Noam Shazeer, Niki Parmar, Jakob Uszkoreit, Llion Jones, Aidan N Gomez, Łukasz Kaiser, and Illia Polosukhin. Attention is All you Need. In *Advances in Neural Information Processing Systems*, volume 30, 2017.
- [60] Zhou Wang, A.C. Bovik, H.R. Sheikh, and E.P. Simoncelli. Image quality assessment: From error visibility to structural similarity. *IEEE Transactions on Image Processing*, 13:600–612, 2004.
- [61] Lauren Watson, Chuan Guo, Graham Cormode, and Alexandre Sablayrolles. On the Importance of Difficulty Calibration in Membership Inference Attacks. In *International Conference on Learning Representations*, 2022.
- [62] Saining Xie, Ross Girshick, Piotr Dollár, Zhuowen Tu, and Kaiming He. Aggregated Residual Transformations for Deep Neural Networks. In *2017 IEEE Conference on Computer Vision and Pattern Recognition (CVPR)*, pages 5987–5995, 2017.
- [63] Zhilin Yang, Zihang Dai, Yiming Yang, Jaime Carbonell, Russ R Salakhutdinov, and Quoc V Le. XLNet: Generalized Autoregressive Pretraining for Language Understanding. In *Advances in Neural Information Processing Systems*, volume 32, 2019.
- [64] Jiayuan Ye, Aadyaa Maddi, Sasi Kumar Murakonda, Vincent Bindschaedler, and Reza Shokri. Enhanced Membership Inference Attacks against Machine Learning Models. In *Proceedings of the 2022 ACM SIGSAC Conference on Computer and Communications Security*, pages 3093–3106, 2022.
- [65] Hongxu Yin, Arun Mallya, Arash Vahdat, Jose M. Alvarez, Jan Kautz, and Pavlo Molchanov. See Through Gradients: Image Batch Recovery via GradInversion. In *Proceedings of the IEEE/CVF Conference on Computer Vision and Pattern Recognition*, pages 16337–16346, 2021.
- [66] Li Yuan, Yunpeng Chen, Tao Wang, Weihao Yu, Yujun Shi, Zihang Jiang, et al. Tokens-to-Token ViT: Training Vision Transformers from Scratch on ImageNet. In *2021 IEEE/CVF International Conference on Computer Vision (ICCV)*, pages 538–547, 2021.
- [67] Guangsheng Zhang, Bo Liu, Tianqing Zhu, Ming Ding, and Wanlei Zhou. Label-Only Membership Inference Attacks and Defenses In Semantic Segmentation Models. *IEEE Transactions on Dependable and Secure Computing*, pages 1–1, 2022.
- [68] Guangsheng Zhang, Bo Liu, Tianqing Zhu, Andi Zhou, and Wanlei Zhou. Visual privacy attacks and defenses in deep learning: A survey. *Artificial Intelligence Review*, 55:4347–4401, 2022.
- [69] Richard Zhang, Phillip Isola, Alexei A. Efros, Eli Shechtman, and Oliver Wang. The Unreasonable Effectiveness of Deep Features as a Perceptual Metric. In *2018 IEEE/CVF Conference on Computer Vision and Pattern Recognition*, pages 586–595, 2018.
- [70] Rui Zhang, Song Guo, Junxiao Wang, Xin Xie, and Dacheng Tao. A Survey on Gradient Inversion: Attacks, Defenses and Future Directions. In *Thirty-First International Joint Conference on Artificial Intelligence*, volume 6, pages 5678–5685, 2022.
- [71] Benjamin Zi Hao Zhao, Aviral Agrawal, Catisha Coburn, Hassan Jameel Asghar, Raghav Bhaskar, et al. On the (In)Feasibility of Attribute Inference Attacks on Machine Learning Models. In *2021 IEEE European Symposium on Security and Privacy (EuroS&P)*, pages 232–251, 2021.
- [72] Bo Zhao, Konda Reddy Mopuri, and Hakan Bilen. iDLG: Improved Deep Leakage from Gradients. *arXiv preprint arXiv:2001.02610*, 2020.
- [73] Ligeng Zhu, Zhijian Liu, and Song Han. Deep Leakage from Gradients. *Advances in Neural Information Processing Systems*, 32, 2019.
- [74] Yang Zou, Zhikun Zhang, Michael Backes, and Yang Zhang. Privacy Analysis of Deep Learning in the Wild: Membership Inference Attacks against Transfer Learning. *arXiv preprint arXiv:2009.04872*, 2020.

A Additional Experimental Results for Membership Inference Attacks



(a) Loss distributions on ResNet-50 (b) Loss distributions on Swin-T

Figure 12: The loss distributions of membership inference attacks against ResNet-50 and Swin-T on CIFAR10.

We plot the loss distributions between the member and non-member data for both CNNs and Transformers in Figure 12. We can see that the distributions of member and non-member data for CNNs are more concentrated at 0, and the distributions for Transformers are concentrated at 0.5. This is why the attacks against CNNs and Transformers have different performances.

B Detailed Architecture Specifications for Experiments

We present a detailed architecture comparison between models from 14 steps (changing from ResNet-50 to ConvNeXt-T) in Table 9. Changes are marked in bold.

Table 9: Detailed Architecture Specifications for 14 steps in Section 5.2.

	ResNet-50, Step 1	Step 2	Step 3	Step 4	Step 5
stem	$7 \times 7, 64$, stride 2 3×3 , max pool, stride 2	$7 \times 7, \mathbf{96}$, stride 2 3×3 , max pool, stride 2	$7 \times 7, 96$, stride 2 3×3 , max pool, stride 2	$\mathbf{4 \times 4, 96}$, stride $\mathbf{4}$ 3×3 , max pool, stride 2	$4 \times 4, 96$, stride 4 3×3 , max pool, stride 2
block1	$[1 \times 1, 64]$ $3 \times 3, 64$ $1 \times 1, 256] \times 3$	$[1 \times 1, \mathbf{96}]$ $3 \times 3, \mathbf{96}$ $1 \times 1, \mathbf{384}] \times 3$	$[1 \times 1, 96]$ $3 \times 3, 96$ $1 \times 1, 384] \times 3$	$[1 \times 1, 96]$ $3 \times 3, 96$ $1 \times 1, 384] \times 3$	$[1 \times 1, 96]$ $\mathbf{d3} \times 3, 96$ $1 \times 1, 384] \times 3$
block2	$[1 \times 1, 128]$ $3 \times 3, 128$ $1 \times 1, 512] \times 4$	$[1 \times 1, \mathbf{192}]$ $3 \times 3, \mathbf{192}$ $1 \times 1, \mathbf{768}] \times 4$	$[1 \times 1, 192]$ $3 \times 3, 192$ $1 \times 1, 768] \times 3$	$[1 \times 1, 192]$ $3 \times 3, 192$ $1 \times 1, 768] \times 3$	$[1 \times 1, 192]$ $\mathbf{d3} \times 3, 192$ $1 \times 1, 768] \times 3$
block3	$[1 \times 1, 256]$ $3 \times 3, 256$ $1 \times 1, 1024] \times 6$	$[1 \times 1, \mathbf{384}]$ $3 \times 3, \mathbf{384}$ $1 \times 1, \mathbf{1536}] \times 6$	$[1 \times 1, 384]$ $3 \times 3, 384$ $1 \times 1, 1536] \times 9$	$[1 \times 1, 384]$ $3 \times 3, 384$ $1 \times 1, 1536] \times 9$	$[1 \times 1, 384]$ $\mathbf{d3} \times 3, 384$ $1 \times 1, 1536] \times 9$
block4	$[1 \times 1, 512]$ $3 \times 3, 512$ $1 \times 1, 2048] \times 3$	$[1 \times 1, \mathbf{768}]$ $3 \times 3, \mathbf{768}$ $1 \times 1, \mathbf{3072}] \times 3$	$[1 \times 1, 768]$ $3 \times 3, 768$ $1 \times 1, 3072] \times 3$	$[1 \times 1, 768]$ $3 \times 3, 768$ $1 \times 1, 3072] \times 3$	$[1 \times 1, 768]$ $\mathbf{d3} \times 3, 768$ $1 \times 1, 3072] \times 3$
other specs	ReLU, BN	ReLU, BN	ReLU, BN	ReLU, BN	ReLU, BN
-	-	-	-	-	-
	Step 6	Step 7	Step 8	Step 9	Step 10
stem	$4 \times 4, 96$, stride 4 3×3 , max pool, stride 2	$4 \times 4, 96$, stride 4 3×3 , max pool, stride 2	$4 \times 4, 96$, stride 4 (removed)	$4 \times 4, 96$, stride 4	$4 \times 4, 96$, stride 4
block1	$[1 \times 1, 96]$ $\mathbf{d3} \times 3, \mathbf{384}$ $1 \times 1, \mathbf{96}] \times 3$	$[\mathbf{d7} \times 7, 96]$ $1 \times 1, 384$ $1 \times 1, 96] \times 3$	$[\mathbf{d7} \times 7, 96]$ $1 \times 1, 384$ $1 \times 1, 96] \times 3$	$[\mathbf{d7} \times 7, 96]$ $1 \times 1, 384$ $1 \times 1, 96] \times 3$	$[\mathbf{d7} \times 7, 96]$ $1 \times 1, 384$ $1 \times 1, 96] \times 3$
block2	$[1 \times 1, 192]$ $\mathbf{d3} \times 3, \mathbf{768}$ $1 \times 1, \mathbf{192}] \times 3$	$[\mathbf{d7} \times 7, 192]$ $1 \times 1, 768$ $1 \times 1, 192] \times 3$	$[\mathbf{d7} \times 7, 192]$ $1 \times 1, 768$ $1 \times 1, 192] \times 3$	$[\mathbf{d7} \times 7, 192]$ $1 \times 1, 768$ $1 \times 1, 192] \times 3$	$[\mathbf{d7} \times 7, 192]$ $1 \times 1, 768$ $1 \times 1, 192] \times 3$
block3	$[1 \times 1, 384]$ $\mathbf{d3} \times 3, \mathbf{1536}$ $1 \times 1, \mathbf{384}] \times 9$	$[\mathbf{d7} \times 7, 384]$ $1 \times 1, 1536$ $1 \times 1, 384] \times 9$	$[\mathbf{d7} \times 7, 384]$ $1 \times 1, 1536$ $1 \times 1, 384] \times 9$	$[\mathbf{d7} \times 7, 384]$ $1 \times 1, 1536$ $1 \times 1, 384] \times 9$	$[\mathbf{d7} \times 7, 384]$ $1 \times 1, 1536$ $1 \times 1, 384] \times 9$
block4	$[1 \times 1, 768]$ $\mathbf{d3} \times 3, \mathbf{3072}$ $1 \times 1, \mathbf{768}] \times 3$	$[\mathbf{d7} \times 7, 768]$ $1 \times 1, 3072$ $1 \times 1, 768] \times 3$	$[\mathbf{d7} \times 7, 768]$ $1 \times 1, 3072$ $1 \times 1, 768] \times 3$	$[\mathbf{d7} \times 7, 768]$ $1 \times 1, 3072$ $1 \times 1, 768] \times 3$	$[\mathbf{d7} \times 7, 768]$ $1 \times 1, 3072$ $1 \times 1, 768] \times 3$
other specs	ReLU, BN	ReLU, BN	ReLU, BN	GELU , BN	Fewer GELU , BN
-	-	-	-	-	-
	Step 11	Step 12	Step 13	ConvNeXt-T, Step 14	
stem	$4 \times 4, 96$, stride 4	$4 \times 4, 96$, stride 4	$4 \times 4, 96$, stride 4	$4 \times 4, 96$, stride 4	
block1	$[\mathbf{d7} \times 7, 96]$ $1 \times 1, 384$ $1 \times 1, 96] \times 3$	$[\mathbf{d7} \times 7, 96]$ $1 \times 1, 384$ $1 \times 1, 96] \times 3$	$[\mathbf{d7} \times 7, 96]$ $1 \times 1, 384$ $1 \times 1, 96] \times 3$	$[\mathbf{d7} \times 7, 96]$ $1 \times 1, 384$ $1 \times 1, 96] \times 3$	
sep ds			$\mathbf{2 \times 2, 192, stride 2}$	$2 \times 2, 192, stride 2$	
block2	$[\mathbf{d7} \times 7, 192]$ $1 \times 1, 768$ $1 \times 1, 192] \times 3$	$[\mathbf{d7} \times 7, 192]$ $1 \times 1, 768$ $1 \times 1, 192] \times 3$	$[\mathbf{d7} \times 7, 192]$ $1 \times 1, 768$ $1 \times 1, 192] \times 3$	$[\mathbf{d7} \times 7, 192]$ $1 \times 1, 768$ $1 \times 1, 192] \times 3$	
sep ds			$\mathbf{2 \times 2, 384, stride 2}$	$2 \times 2, 384, stride 2$	
block3	$[\mathbf{d7} \times 7, 384]$ $1 \times 1, 1536$ $1 \times 1, 384] \times 9$	$[\mathbf{d7} \times 7, 384]$ $1 \times 1, 1536$ $1 \times 1, 384] \times 9$	$[\mathbf{d7} \times 7, 384]$ $1 \times 1, 1536$ $1 \times 1, 384] \times 9$	$[\mathbf{d7} \times 7, 384]$ $1 \times 1, 1536$ $1 \times 1, 384] \times 9$	
sep ds			$\mathbf{2 \times 2, 768, stride 2}$	$2 \times 2, 768, stride 2$	
block4	$[\mathbf{d7} \times 7, 768]$ $1 \times 1, 3072$ $1 \times 1, 768] \times 3$	$[\mathbf{d7} \times 7, 768]$ $1 \times 1, 3072$ $1 \times 1, 768] \times 3$	$[\mathbf{d7} \times 7, 768]$ $1 \times 1, 3072$ $1 \times 1, 768] \times 3$	$[\mathbf{d7} \times 7, 768]$ $1 \times 1, 3072$ $1 \times 1, 768] \times 3$	
other specs	Fewer GELU , Fewer BN	Fewer GELU , Fewer LN Conv w/ True bias	Fewer GELU , Fewer LN Conv w/ True bias	Fewer GELU , Fewer LN Conv w/ True bias Stochastic depth , Layer Scale	